EFFECT OF CHEMISTRY MODIFICATIONS AND HEAT TREATMENTS ON THE MECHANICAL PROPERTIES OF DS MAR-M200 SUPERALLOY

Zheng Yunrong*, Wang Yuping*, Xie Jizhou*,
Pierre Caron**, and Tasadduq Khan**

*Institute of Aeronautical Materials, Beijing (BIAM)
**Office National d'Etudes et de Recherches Aerospatiales (ONERA)

Abstract

Hf and Zr can promote the formation of eutectic ($\gamma+\gamma'$), MC_2, and Ni_5M phases. In the alloy with equal atomic percent Zr and Hf, the solubility of Zr in eutectic γ' is lower than that of Hf, and Zr content in Ni_5M is much higher than Hf. This distribution of Zr is beneficial to the formation of Ni_5M and lowers the strengthening efficiency of Zr. A pretreatment of 1130°C/3hr efficiently eliminates Ni_5M and, as a consequence, increases the incipient melting temperature of the alloy. The precipitation treatment of 1100°C/4hr leads to cuboidal γ' precipitation of about 0.5 μm size and causes the Hf-containing alloy to have a much higher creep strength than the Hf-free alloy in the temperature range of 760 to 1050°C. The Hf-containing alloy showed greater LCF (low cycle fatigue) life in comparison to the Hf-free alloy. A similar tendency was found when Zr was either partially or totally substituted for Hf. A higher rate of solidification facilitates enhanced LCF life due to a finer structure and more perfect orientation. Surface slip analysis showed that intersection of two sets of slip in adjacent grains occurred in the Hf-free and Hf-containing alloys, but cracking at the columnar grain boundary easily took place in the Hf-free alloy. The number of surface cracks of LCF specimens and their length per unit area are much higher in the Mar-M200 alloy. MC cracking preferentially occurs at long rod-shaped carbides perpendicular to the stress axis, and then propagates through the interdendritic region. The Hf-containing alloy cracks along the crystallographic planes by separation of slip bands.

Superalloys 1988
Edited by S. Reichman, D.N. Duhl,
G. Maurer, S. Antolovich and C. Lund
The Metallurgical Society, 1988

Introduction

Mar-M200 is an early superalloy which has good high temperature strength; however, it was found that premature rupture of this alloy occurred at intermediate temperature. Later, a potential problem (i.e., "ductility valley") that occurs with many high-strength cast superalloys at intermediate temperature was recognized. Hafnium (Hf) additions and directional solidification techniques were considered as better ways to solve this problem. Directionally solidified (DS) superalloys were first introduced by Pratt & Whitney for military engines in the late 1960's and for commercial engines around 1974. Since that time, effort was devoted more specifically to the development of single crystal (SC) superalloys because it was thought that no significant improvement in properties was possible with the DS alloys. In spite of the advances made in the development of new SC alloys, attention has been rediverted toward the DS alloys for economic and technical reasons.

As we know, Hf improves transverse mechanical properties of DS superalloys, but makes stress-rupture life above 980°C drop (1). In order to overcome this disadvantage, a modified heat treatment (2) suitable for SC superalloys was introduced into DS Mar-M200+Hf. On the other hand, Zr and Hf have similar alloying behavior (3); and recent work (4) has proved that Zr can be substituted for Hf. Accordingly, BIAM and ONERA conducted a joint program to explore the effect of Hf and Zr additions, as well as a modified heat treatment, on the tensile, creep, and fatigue strength of the DS Mar-M200 superalloy. This paper describes some of the results, with particular emphasis on the low cycle fatigue behavior of such alloys.

Experimental Procedures

The Mar-M200 alloy and its modified versions (Hf and/or Zr) were cast into master ingots at BIAM. Their chemical compositions are listed in Table I. A number of DS rods were then prepared at both BIAM and ONERA. The former used a ISP2/III DS furnace and the latter did a high gradient DS set. The high rate solidification process used at BIAM results in a cooling rate (gradient x withdrawal rate) of 25°C/min, whereas the cooling rate at ONERA was 10°C/min. Various heat treatments were used for the different alloys (Table II). Pretreatment of 1130°C/3hr for Zr-containing alloys was performed to eliminate existing Ni_5Zr phase in order to increase the incipient melting temperature of the alloy. Microstructural analysis of as-cast and heat treated specimens was conducted using an optical microscope, SEM, and EPMA.

Table I. Chemical Composition of Alloys

Alloy	Cr	Co	Al	Ti	Nb	W	Hf	C	B	Zr	Ni
Mar-M200	8.56	9.80	5.05	2.03	1.03	11.20	--	0.15	0.015	0.0003	base
Mar-M200+Hf	8.88	9.95	5.13	2.16	1.02	12.20	1.78	0.13	0.015	0.035	base
Mar-M200+Zr	8.56	9.80	5.05	2.03	1.03	11.20	--	0.15	0.015	0.70	base
Mar-M200+Zr +Hf	8.56	9.80	5.05	2.03	1.03	11.20	0.80	0.15	0.015	0.40	base

Tensile and creep tests were performed at a temperature range of 20 to 1050°C, and specimens were machined into standard cylindrical bars. A large number of fully reversed strain-controlled LCF tests (R=-1, frequency 0.33 Hz, total strain range 1.0 to 1.4%) were performed on a MTS servo-hydraulic fatigue testing machine for various DS alloys at 760°C by using cylindrical

and plate specimens. The plate specimens were prepolished before testing in order to reveal slip trace and crack initiation sites. Some LCF tests were interrupted at different cycles before failure for transmission electron microscopic and metallographic analysis to understand the effect of Hf on deformation mechanisms and crack initiation. For ruptured specimens, fracture surfaces were observed by SEM.

Experimental Results

Microstructure of Alloys

As-Cast Microstructure. Specimens given rapid solidification have a finer dendritic structure. Results of quantitative metallography have shown that the dendritic densities of BIAM and ONERA bars are $1391/cm^2$ and $706/cm^2$, respectively. The directional diversion from (001) is less than 6° and 16° for BIAM and ONERA bars. In the as-cast Mar-M200 alloy, there are MC carbide, eutectic ($\gamma+\gamma'$), and minor M_3B_2 and M_2SC phases. In addition to these phases, there are also MC_2 and Ni_5M in the Hf- and/or Zr-containing alloys. Both elements promote the formation of eutectic ($\gamma+\gamma'$) and the intermetallic compound Ni_5M. Moreover, the effect of Zr is more intense. The volume percents of eutectic ($\gamma+\gamma'$) and Ni_5Hf in the Hf-containing alloy are 10.53 and 0.23%, whereas eutectic ($\gamma+\gamma'$) and Ni_5Zr in the Zr-additive alloy are 10.38 and 0.71%. Ni_5Zr appears around eutectic ($\gamma+\gamma'$) and in cellular form (Fig. 1), as does Ni_5Hf. Hf and Zr can change script MC carbide into blocky carbides, but they cannot influence the amount of MC carbide distinctly.

The composition of some phases was measured by EPMA, and the results are listed in Table III. The composition of MC only represents the metallic 'M' half of the carbide. Table III shows that in an alloy with equal atomic percent of Zr and Hf, the solubility of Zr in eutectic γ' is lower than that of Hf, and the Zr content in Ni_5M is much higher than Hf. The above characterization promotes the formation of Ni_5Zr in Zr-containing alloys. This implies that we cannot substitute Zr for Hf in the same atomic fraction, and a rather low content of Zr is beneficial.

Heat Treated Microstructure. A pretreatment of 1130°C/3hr is performed to promote the transformation of Ni_5Zr into MC_2 and to restrict incipient melting during solution treatment. After 1130°C/3hr, Zr-rich MC_2 formed around the eutectic ($\gamma+\gamma'$) (Fig. 2). The 1230°C/2hr treatment is basically a full solid solution treatment for Mar-M200, but treatment in the temperature range of 1205 to 1225°C gives an incomplete solid solution for the four alloys. During solid solution treatment, secondary MC_2 is scattered in the vicinity of the eutectic ($\gamma+\gamma'$) (Fig. 3). Precipitation treatment at 1100°C/4hr leads to cuboidal γ' of about 0.5 μm.

Tensile and Creep Properties

Ultimate tensile strength (UTS), 0.2% yield strength (YS), and creep life were measured (Tables IV and V). Table IV shows that both alloys have almost the same UTS, 0.2% YS, and elongation in the temperature range of R.T. to 760°C; but at higher temperature (950°C), these properties in the Hf-containing alloy are rather higher than those in the Hf-free alloy. The effect of heat treatment is not obvious in both alloys.

It can be seen in Table V that the Hf-containing alloy has much longer rupture life than that of the Hf-free alloy in the temperature range of 760 to 1050°C. Previous investigation indicated that Hf additions to the DS Mar-M200 alloy improved the transverse stress-rupture life and elongation at intermediate temperature; however, Hf is not beneficial at high temperature, especially above 1000°C in an alloy given an incomplete solid solution treatment. The present work shows that by using heat treatments II and III, satisfactory results can be obtained.

Table II. Heat Treatment (H.T.) of Alloys

H.T.	Temperature/Time	Application
I	1205°C/2hr, A.C.+870°C/32hr, A.C.	Mar-M200 Mar-M200+Hf
II	1230°C/2hr, A.C.+1100°C/4hr, A.C. +870°C/20hr, A.C.	Mar-M200
III	1225°C/2hr, A.C.+1100°C/4hr, A.C. +870°C/20hr, A.C.	Mar-M200+Hf
IV	1130°C/3hr, A.C.+1210°C/3hr, A.C. +1100°C/4hr, A.C.+870°C/20hr, A.C.	Mar-M200+Zr
V	1130°C/3hr, A.C.+1220°C/3hr, A.C. +1100°C/4hr, A.C.+870°C/20hr, A.C.	Mar-M200+Zr+Hf

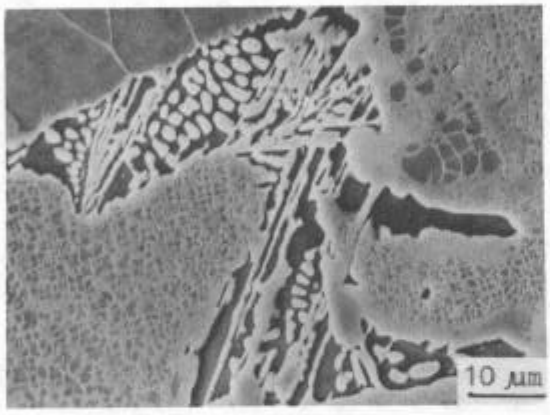

Figure 1 - Morphology of Ni_5Zr in Mar-M200+Zr.

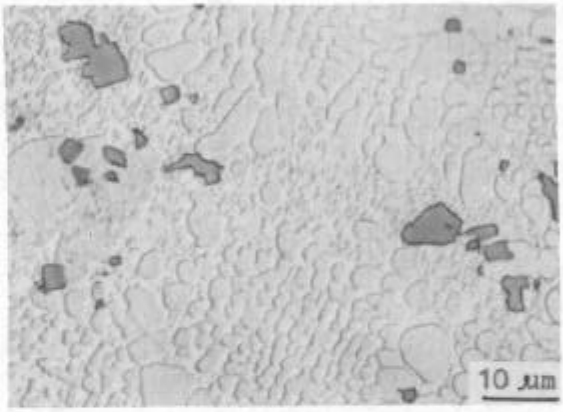

Figure 2 - Zr-rich MC_2 in Mar-M200+Zr.

Low Cycle Fatigue (LCF) Properties

Figure 4 shows the results of axial tension-compression LCF tests for both alloys. As shown, the Hf-containing alloy has a longer fatigue life. The life of some specimens of the Hf-containing alloy is longer by about one order of magnitude than the Hf-free alloy, and BIAM bars have longer lives than ONERA bars due to the different directionally solidified conditions.

A similar tendency was found when Zr was either partially or totally substituted for Hf. The role of Zr in improving LCF is not as distinct as Hf, but the Zr-containing alloy is better than the Hf-free alloy in LCF.

Observation of LCF Cracking

Systematic observation was conducted for a set of plate specimens at 760°C, 1.4% total strain range, and 0.33 Hz. The number N and length L of surface cracks per unit area as well as the average length were measured for about half life and ruptured specimens. The results are listed in Table VI. It was found that the cracking tendency of the Hf-containing alloy is

Table III. Phase Composition in Alloy, Atomic %

Alloy	Phase	Ti	Al	Cr	Ni	W	Co	Nb	
Mar-M200	MC_1 *	43.29	0.10	1.85	6.84	13.92	0.97	32.16	
	Eutectic γ'	4.68	13.02	5.49	66.84	1.42	7.84	0.68	
Mar-M200 + 0.60Hf	MC_1 *	40.52	0.07	1.30	5.96	14.19	0.95	26.46	1
	MC_2 *	21.74	0.40	2.24	10.26	6.29	2.18	19.47	3
	Ni_5Hf	4.53	1.65	5.14	61.88	1.41	9.05	1.93	1
	Eutectic γ'	3.70	11.95	7.15	64.01	2.07	8.70	0.70	
Mar-M200 + 0.45Zr	MC_1 *	47.77	0.00	0.96	3.41	13.91	0.42	26.88	
	MC_2 *	11.30	0.18	1.45	7.95	5.84	1.33	21.93	
	Ni_5Zr	0.71	1.59	2.25	66.19	0.26	7.05	0.53	
	Eutectic γ'	4.61	11.91	4.96	67.73	1.72	7.49	0.62	
Mar-M200 + 0.26Zr+0.27Hf	MC_1 *	43.82	0.06	0.91	3.92	13.28	0.54	27.39	
	MC_2 *	19.23	0.05	1.26	7.42	6.54	1.39	21.80	2
	Ni_5(Zr, Hf)	1.79	2.45	2.79	67.24	0.44	7.42	0.43	
	Eutectic γ'	3.54	13.63	6.55	63.98	2.07	8.19	0.50	

* Composition of MC only represents metallic radical 'M'

Table IV. Tensile Properties of DS Mar-M200 Alloy

Temperature °C	D. S. Condition	Hf-free alloy H. T.	0.2%Y.S. (MPa)	U.T.S (MPa)	δ (%)	ψ (%)	Hf-containir H. T.	0.2%Y.S (MPa)	U.T. (MPa
		II	1007	1115	5.85		III	1024	1217
R. T.	BIAM	I	1001	1197			I	1091	1284
		I	989	1238	10.8	13.5	I	1106	1256
650	BIAM	II	927	1119	11.1		III	977	1173
		II	1030	1109	6.5		III	1078	1121
760	BIAM	I	967	1205	8.8	14.0	I	1091	1317
		I	990	1227	9.2	14.5	I	1106	1332
	ONERA	I	886	1107	6.2	7.0	I	920	1118
950	BIAM	II	437	559	16.1		III	555	641

Table V. Creep Properties of DS Mar-M200 Alloy

Test Conditions Temperature °C	Stress (MPa)	Hf-free alloy H.T.	Time for 1% creep (h)	Rupture life (h)	Elongation (%)	H.T	Hf-containi Time for 1% creep (h)	R
760	750	II	13	351	8.6	III	5	
850	450	II	45	197	19.6	III	162	
950	200	II	125	251	6.8	III	228	
1050	100	II	104	173	13.6	III	156	

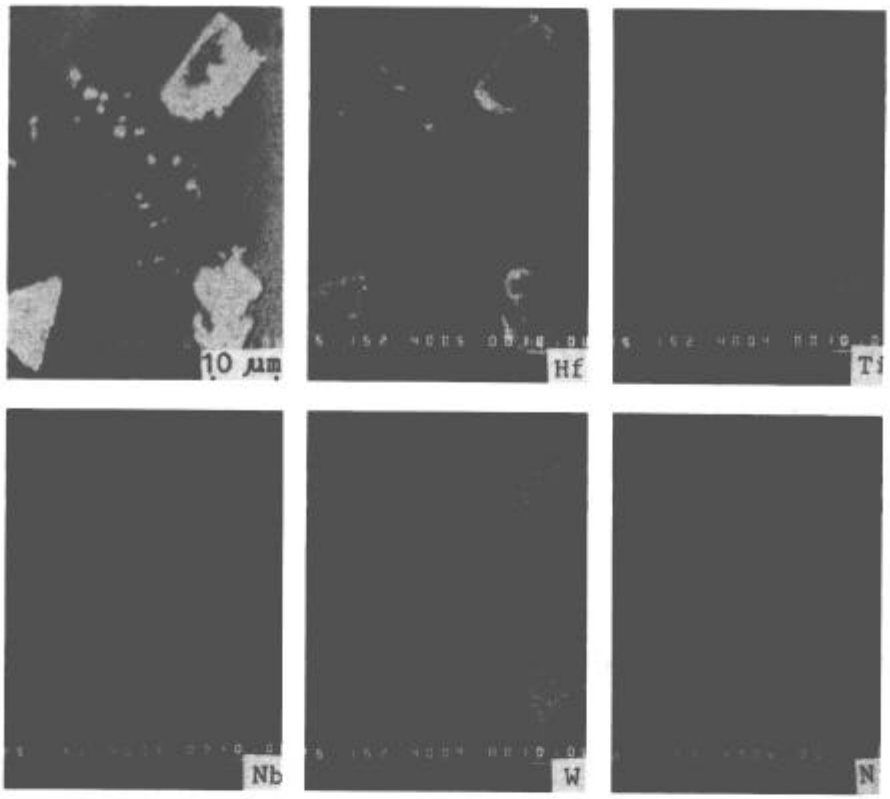

Figure 3 - Element distribution in MC_2 for Mar-M200+Hf after heat treatment I.

Table VI. Strain-Controlled LCF Results for Plate Specimens

Alloy	Specimen No.	Cycle Nf	Result	Density of Cracks N/mm^2	Length of Cracks $L(mm/mm^2)$	Average Length $\bar{L}(mm)$
Mar-M	4T	21	unruptured	2.30	0.12	0.0534
200	6B	57	ruptured	3.89	0.22	0.0561
Mar-M	3T	203	unruptured	0	0	0
200+Hf	3B	315	ruptured	0.07	0.0064	0.0875

very low. After testing, the surface of the Mar-M200 specimens was rougher due to deformation than that of Mar-M200+Hf. Surface slip analysis showed that intersection of two sets of slip bands in adjacent grains occurred at the columnar grain boundary. For Mar-M200, microcracks preferentially formed (Fig. 5). Although similar slip band intersections took place in Mar-M200+Hf, the grain boundaries did not crack. The cracking pattern of both alloys is much different within the grains. Mar-M200 has predominantly interdendritic cracks (Fig. 6a), but Mar-M200+Hf has interdendritic and transdendritic cracks. The latter is very flat with straight segments having some steps, as shown by the arrow in Figure 6b. It means that this kind of crack is related to crystallographic cracking caused by slip. At high strain amplitude, extensive MC cracking was observed in the Hf-free alloy during the first few cycles. The MC cracking preferentially occurs at long rod-shaped carbides perpendicular to the stress axis (Fig. 7a). The Hf-containing alloy has higher resistance to MC cracking due to the presence of blocky carbides. Even if some carbides crack, the crack size is very small (Fig. 7b).

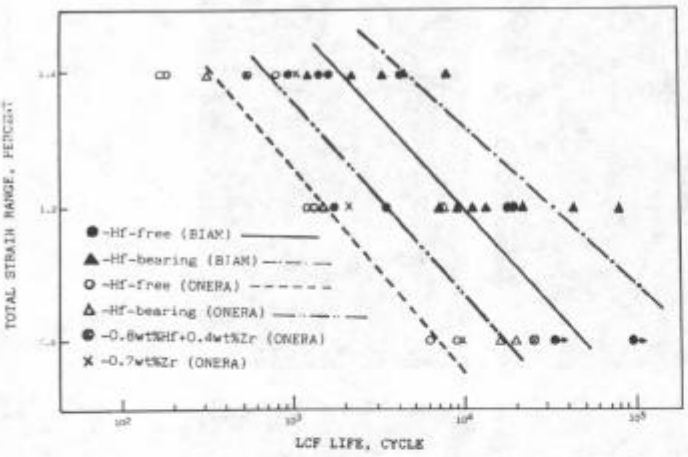

Figure 4 - LCF properties of alloys.

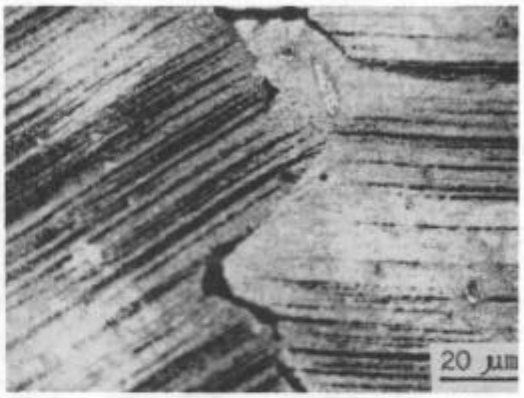

Figure 5 - Intersection of two sets of slip in specimen 6B.

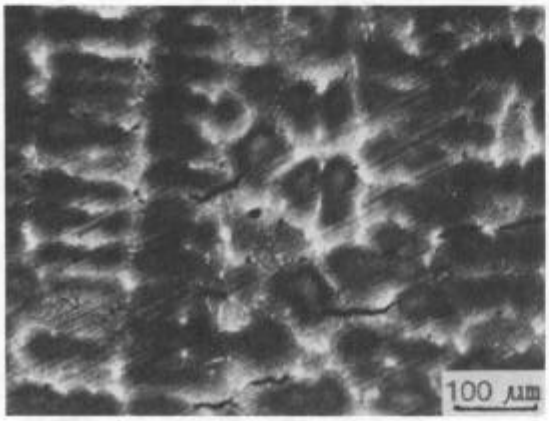

a)

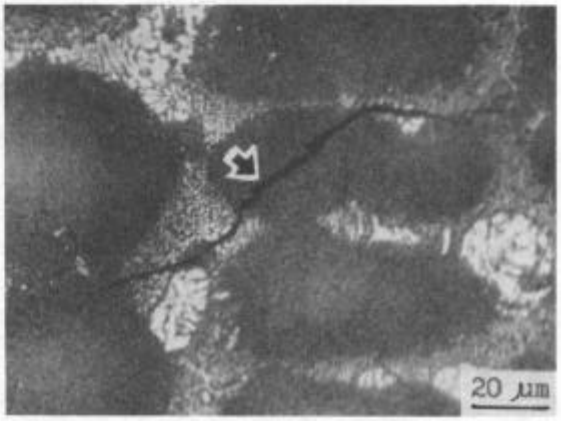

b)

Figure 6 - Intragranular cracking pattern of two alloys: (a) specimen 6B, and (b) specimen 3B.

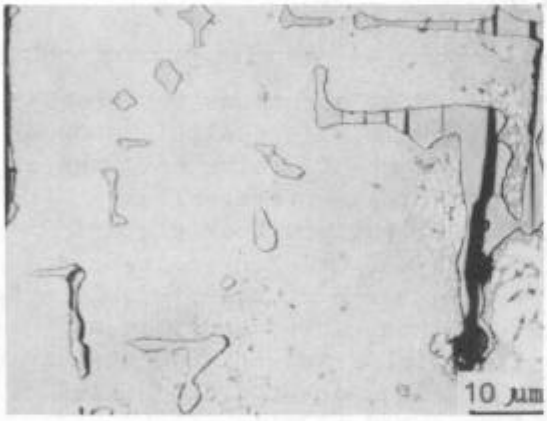

a)

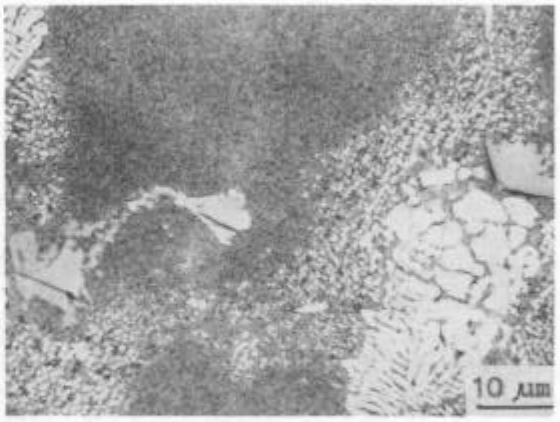

b)

Figure 7 - MC carbide cracking of Hf-containing and Hf-free alloy: (a) specimen 6B, and (b) specimen 3T.

The microscopic characterization of fatigue rupture is very different for the two alloys. At the fracture surface of Mar-M200, the following pattern often exists: a cluster of MC carbides crack which then propagates through the interdendritic region, as clearly indicated by the fatigue striation and stops at dendritic arms (Fig. 8a). In the late period of fatigue, dendrites are separated by a number of local fatigue cracking zones. In the Hf-containing alloy, cracking takes place along the crystallographic plane of heavy slipping and the fracture surface appears to be a flat zone corresponding to the segment shown by the arrow in Figure 6b. On the flat fracture, there are some slip bands (Fig. 8b).

A TEM examination of thin foils taken from the fatigue specimens was carried out. The results showed that there were a lot of stacking faults caused by long distance slip in the Hf-free alloy (Fig. 9a), but dislocations were difficult to spread into a stacking fault and prone to twining in the Mar-M200+Hf alloy (Fig. 9b). This demonstrated that the Hf-containing alloy had more uniform deformation than the Hf-free alloy. The effect of Zr on the LCF deformation mechanism is very similar to Hf.

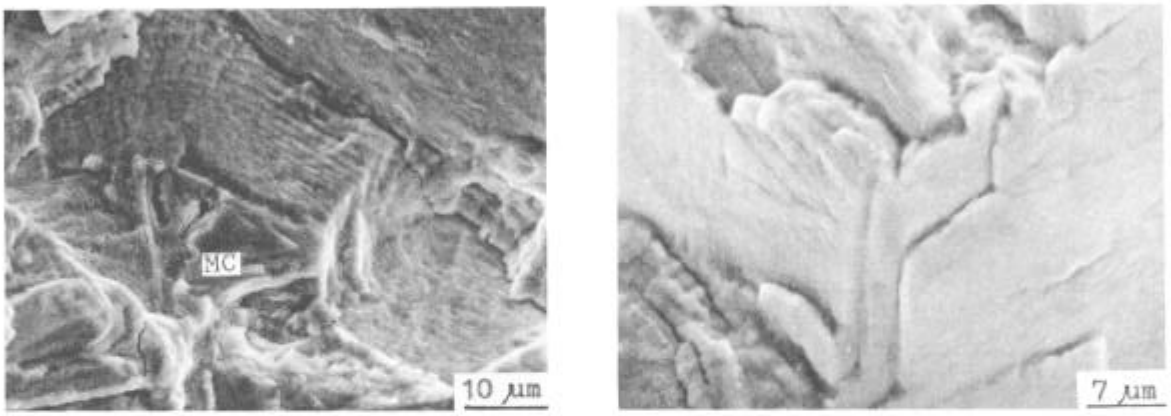

a) b)

Figure 8 - Fatigue fracture surface of two alloys: (a) specimen 6B, and (b) specimen 3B.

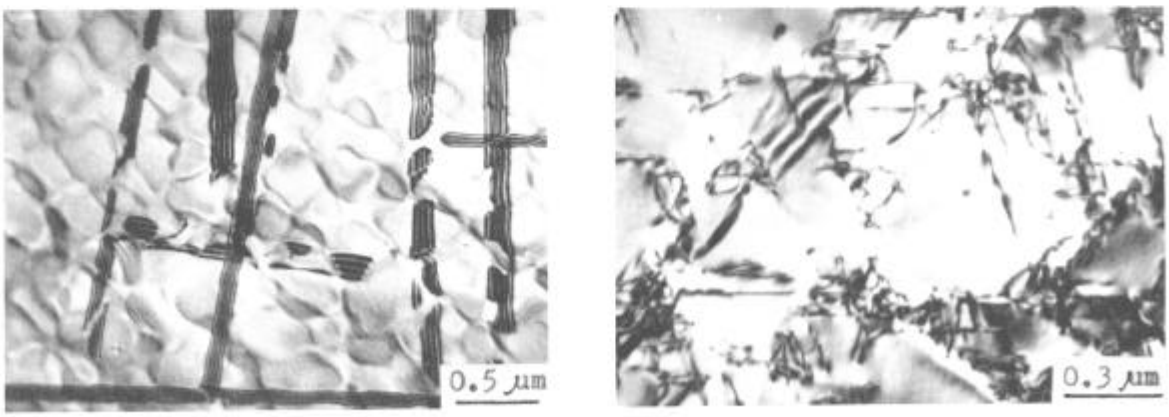

a) b)

Figure 9 - Dislocation structure in both alloys: (a) Mar-M200, ϵt=1.2%, 1700 cycles; and (b) Mar-M200+Hf, ϵt=1.2%, 44484 cycles.

Conclusions

1. Both Hf and Zr can promote the formation of eutectic γ', MC_2, and Ni_5M phases. Zr promotes the formation of Ni_5M to a greater extent than Hf. The solubility of Zr in Ni_5M is higher than that of Hf, but its solubility in γ' is lower than Hf. As a result, the strengthening efficiency of Zr is not as strong as Hf.

2. Ni_5Zr in a Zr-containing alloy can be eliminated by pretreatment at 1130°C/3hr; therefore, incipient melting can be avoided below 1235°C.

3. The Hf-containing alloy showed greater LCF life compared to the Hf-free alloy. A similar tendency was found when Zr was either partially or totally substituted for Hf. High rate solidification enhances LCF life further.

4. The creep life for DS Mar-M200+Hf at 760°C and 1050°C was increased with a 1225°C/2hr + 1100°C/4hr + 870°C/20hr heat treatment.

5. The number of surface cracks in LCF specimens and their length per unit area are much higher in the Hf-free alloy. The cracks mainly originate from MC carbides, then propagate through the interdendritic region. The Hf-containing alloy cracks along the crystallographic planes. This proved that the Hf-containing alloy has a more uniform deformation mode and higher interdendritic coherent strength.

References

1. Wang Luobao, Chen Rongzhang and Wang Yuping, "Influences of Directionally Solidified Techniques and Hf Content on a Nickel-Base Superalloy," The Production and Application of Less Common Metals, (The Metals Society and Chinese Society of Metals, 1982), Book II, Paper 43, 1-17.

2. T. Khan et al., "Single Crystal Superalloys for Turbine Blades: Characterization and Optimization of CMSX-2 Alloy," (Paper presented at the 11th Symposium on Steels and Special Alloys for Aerospace, Paris Air Show Le Bourget, 6 June 1985).

3. D. N. Duhl, "Enhancement of Transverse Properties of Directionally Solidified Superalloys," USPO 3, 700, 433, Oct. 24, 1972.

4. Zheng Yunrong, Cai Yulin and Ruan Zhongci, "Investigation of Zr as a Substitute for Hf in Cast Ni-Base Superalloys," Acta Metallurgica Sinica, 23(5)(1987), A430-433.